ISSN 1063-7761, Journal of Experimental and Theoretical Physics, 2014, Vol. 119, No. 3, pp. 375–383. © Pleiades Publishing, Inc., 2014.
Original Russian Text © A.P. Anyutin, I.P. Korshunov, A.D. Shatrov, 2014, published in Zhurnal Eksperimental'noi i Teoreticheskoi Fiziki, 2014, Vol. 146, No. 3, pp. 429–438.

ATOMS, MOLECULES, OPTICS

Degeneracy of Low-Frequency Resonances in a Chiral Anisotropically Conducting Cylinder Filled with a Metamaterial

A. P. Anyutin*, I. P. Korshunov, and A. D. Shatrov**

Fryazino Branch, Kotel'nikov Institute of Radio Engineering and Electronics, Russian Academy of Sciences, Fryazino, Moscow oblast, 141190 Russia

**e-mail: anioutine@mail.ru*

***e-mail: korip@ms.ire.rssi.ru*

Received January 16, 2014

Abstract—The paper considers the 2D problem of a cylinder, filled with a metamaterial with anisotropic surface conductivity along helical lines, excited by electric and magnetic field filaments. High-Q resonances occurring in small (as compared to the wavelength) cylinders with a permeability close to -1 are investigated. The effect of degeneracy of oscillations with various values of index m in the $\cos(m\varphi)$ law describing the azimuthal dependence of resonant fields is discovered. The range of parameters in which degenerate oscillations exist is determined. The spatial and polarization structures of magnetic fields are analyzed. An analytic description is proposed for resonant fields in the quasi-static approximation.

DOI: 10.1134/S1063776114080020

1. INTRODUCTION

Electrodynamics of artificial media with negative permittivity ε and permeability μ has rapidly developed in recent years [1–6]. Such artificial media are usually referred to as metamaterials [7]. The electromagnetic fields induced by sources located near the bodies made of metamaterials possess a number of peculiar properties [8]. For example, effects of resonant excitation of electrical- or magnetic-type modes of a sphere were discovered in [9] in analysis of radiation from dipole sources on spherical metamaterial particles. According to [9], if the parameters of the material are close to $\varepsilon = -1 - 1/m$ or $\mu = -1 - 1/m$ ($m = 1, 2, 3, \ldots$), these resonances are quasi-static (i.e., exist in particles with electrically small sizes). Such resonances are not observed in objects made of conventional magnetodielectrics.

Quasi-static high-Q resonances were observed in [10] in cylinders made of metamaterials in which ε or μ are close to -1. Such cylinders can be treated as ring resonators on very slow surface waves propagating along the boundary of a metamaterial. In this case, the field at the resonance frequency is described by a single azimuthal harmonic $\cos(m\varphi)$. The spectral and polarization properties of fields in a multiturn helix filled with a metamaterial were investigated in [11]. The helix was simulated by a surface with an ideal anisotropic conductivity along the helical lines. Surface waves are formed in such a structure by the interface between the media as well as by the wire grid located on this interface. We will show that for certain combinations of the parameters of the problem, degeneracy of quasi-static resonances takes place. It will be demonstrated, in particular, that in some cases the field can be described by the function $\cos(m\varphi)$ with different values of m in the near- and far-field zones.

Among publications in this field, we can also mention [12], which considered radiation emitted by optically active molecules located near spherical particles of chiral metamaterials characterized by three quantities ε, μ, and η (η is the chirality parameter). The features of resonant phenomena determined by negative values of quantities ε and μ and of the chirality of the medium were investigated. In contrast to [12], we will consider cylindrical, not spherical scatterers; the chirality of an object of a metamaterial is determined by the properties of its boundary and not by the properties of the metamaterial constituting it. The helical geometry of conductors is the simplest way to achieve chiral electrodynamic objects of a metamaterial in developing a new elemental base in the decimeter and centimeter wavelength ranges. The 2D nature of the model problem considered here makes it possible to obtain an analytic description of the degeneracy of eigenmodes using a simpler mathematical apparatus.

2. FORMULATION OF THE PROBLEM AND SOLUTION METHOD

We consider the problem of excitation of a circular cylinder made of a metamaterial with parameters ε and μ by a filamentary source. We will use the cylindrical system of coordinates (r, φ, z) (Fig. 1). We assume that the following bilateral boundary conditions of

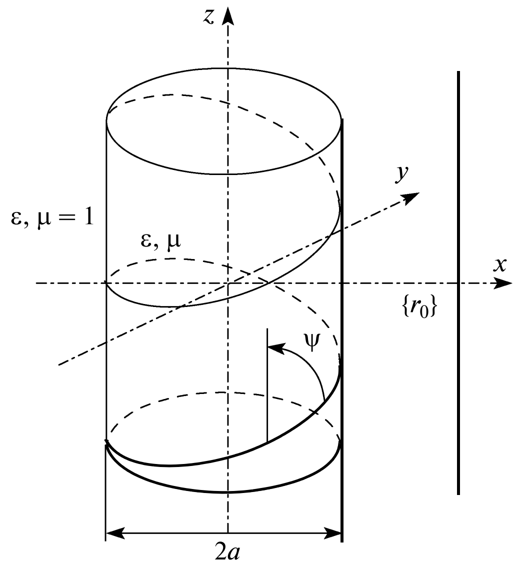

Fig. 1. Geometry of the problem.

ideal anisotropic conductivity along the helical lines hold on the cylinder surface ($r = a$):

$$E_z^+ = E_z^-, \quad E_\varphi^+ = E_\varphi^-, \quad E_z\cos\psi + E_\varphi\sin\psi = 0, \quad (1)$$

$$(H_z^+ - H_z^-)\cos\psi + (H_\varphi^+ - H_\varphi^-)\sin\psi = 0, \quad (2)$$

where the "plus" and "minus" signs correspond to the outer ($r > a$) and inner ($r < a$) surfaces, φ being the twist angle of the helix. For definiteness, we assume that the helical lines are right ($0 < \psi < \pi/2$). The model of the cylindrical surface with anisotropic conductivity of the helical type successfully describes wire (single-turn or multiturn) spirals if the distance between the axes of adjacent conductors are much smaller than the wavelength and the gap spacing lies in a certain interval [13, 14].

The cylinder is excited by electric and magnetic filamentary currents located outside the cylinder at point $r_0 > a$, $\varphi_0 = 0$ (see Fig. 1). We assume that the exciting currents are independent of coordinate z. In this case, the problem under investigation is two-dimensional, but with two potentials. For the potentials, we choose the functions

$$U_1(r, \varphi) = E_z(r, \varphi), \quad U_2(r, \varphi) = H_z(r, \varphi). \quad (3)$$

In further analysis, we will use vector notation, e.g.,

$$\mathbf{U} = \{U_1, U_2\}. \quad (4)$$

Vector function $\mathbf{U}(r, \varphi)$ satisfies the inhomogeneous Helmholtz equation

$$\left[\frac{\partial^2}{\partial r^2} + \frac{1}{r}\frac{\partial}{\partial r} + \frac{1}{r^2}\frac{\partial^2}{\partial\varphi^2} + k^2\varepsilon(r)\mu(r)\right]\mathbf{U}(r, \varphi) = -\frac{4i}{r}\mathbf{A}\delta(r - r_0)\delta(\varphi), \quad (5)$$

where k is the wavenumber in the free space and functions $\varepsilon(r)$ and $\mu(r)$ are defined as

$$\varepsilon(r) = \begin{cases}\varepsilon, & 0 < r < a,\\ 1, & r > a,\end{cases} \qquad \mu(r) = \begin{cases}\mu, & 0 < r < a,\\ 1, & r > a,\end{cases} \quad (6)$$

$\delta(...)$ is the Dirac delta function, and components A_1 and A_2 of vector $\mathbf{A}$ define the amplitudes of the electric and magnetic exciting currents.

Quantities E_φ and H_φ appearing in boundary conditions (1) and (2), as well as the radial components of the electromagnetic field, can be expressed in terms of U_1 and U_2 using the formulas following from the Maxwell equations:

$$E_\varphi = -\frac{1}{ik\varepsilon(r)r}\frac{\partial U_2}{\partial r}, \quad H_\varphi = -\frac{1}{ik\mu(r)r}\frac{\partial U_1}{\partial r}, \quad (7)$$

$$E_r = \frac{1}{ik\varepsilon(r)r}\frac{\partial U_2}{\partial\varphi}, \quad H_r = -\frac{1}{ik\mu(r)r}\frac{\partial U_1}{\partial\varphi}. \quad (8)$$

Field $\mathbf{U}(r, \varphi)$ must also satisfy the radiation condition; i.e., for $kr \longrightarrow \infty$, the field must have the form

$$\mathbf{U}(r, \varphi) = \mathbf{\Phi}(\varphi)\left(\frac{2}{\pi kr}\right)^{1/2}\exp\left(-ikr + \frac{i\pi}{4}\right). \quad (9)$$

Exciting field $\mathbf{U}^0$ is the solution to the inhomogeneous Helmholtz equation in the free space and is defined as

$$\mathbf{U}^0(r, \varphi) = \mathbf{A}H_0^{(2)}\left(k\sqrt{r^2 + r_0^2 - 2rr_0\cos\varphi}\right), \quad (10)$$

where $H_0^{(2)}$ is the Hankel function. The directional pattern of the field has the form

$$\mathbf{\Phi}^0(\varphi) = \mathbf{A}\exp(ikr_0\cos\varphi). \quad (11)$$

The total field $\mathbf{U}$ outside the cylinder is the sum of the exciting ($\mathbf{U}^0$) and scattered ($\mathbf{U}^s$) fields. We will denote by $\Phi^s(\varphi)$ the scattering diagram (i.e., the directional pattern of field $\mathbf{U}^s$).

Equation (5), boundary conditions (1), (2), and radiation condition (9) determine the boundary-value problem for field $\mathbf{U}(r, \varphi)$ completely.

The problem formulated here can be solved analytically by separating variables [11]. We can write the final expressions for the wave fields. We introduce vectors $\mathbf{L}^{(m)}$, $\mathbf{M}^{(m)}$, $\mathbf{N}^{(m)}$ and scalar $W^{(m)}$:

$$\mathbf{L}^{(m)} = \{H_m^{(2)\prime}(ka)\sin\psi, iH_m^{(2)}(ka)\cos\psi\}, \quad (12)$$

$$\mathbf{M}^{(m)} = \{H_m^{(2)\prime}(ka)\sin\psi, -iH_m^{(2)}(ka)\cos\psi\}, \quad (13)$$

$$\mathbf{N}^{(m)} = \left\{\frac{n}{\varepsilon}J_m'(kna)\sin\psi, iJ_m(kna)\cos\psi\right\}, \quad (14)$$

$$W^{(m)} = H_m^{(2)}(ka)J_m(kna)\left[\frac{n}{\varepsilon}H_m^{(2)}(ka)J'_m(kna) - H_m^{(2)\prime}(ka)J_m(kna)\right]\cos^2\psi + \frac{n}{\varepsilon}H_m^{(2)\prime}(ka)J'_m(kna)\left[\frac{n}{\mu}H_m^{(2)}(ka)J'_m(kna) - H_m^{(2)\prime}(ka)J_m(kna)\right]\sin^2\psi, \quad (15)$$

where

$$n = \sqrt{\varepsilon\mu}, \quad (16)$$

$J_m(kna)$ are the Bessel functions, and the prime indicates differentiation with respect to the argument.

Total field $\mathbf{U}(r, \varphi)$ inside the cylinder ($r < a$) can be written in the form

$$\mathbf{U}(r, \varphi) = \sum_{m=0}^{\infty} \delta_m H_m^{(2)}(kr_0)\mathbf{B}^{(m)} J_m(knr)\cos(m\varphi), \quad (17)$$

where

$$\delta_m = \begin{cases} 1, & m = 0, \\ 2, & m \geq 1, \end{cases} \quad (18)$$

$$\mathbf{B}^{(m)} = \frac{2i(\mathbf{A}, \mathbf{M}^{(m)})}{\pi ka W^{(m)}}\mathbf{N}^{(m)}. \quad (19)$$

In expression (19), $(\mathbf{A}, \mathbf{M}^{(m)})$ denotes the scalar product

$$(\mathbf{A}, \mathbf{M}^{(m)}) = A_1 M_1^{(m)} + A_2 M_2^{(m)}. \quad (20)$$

The field outside the cylinder ($r > a$) can be written as the sum of two terms (incident and scattered fields):

$$\mathbf{U}(r, \varphi) = \mathbf{U}^0(r, \varphi) + \mathbf{U}^s(r, \varphi). \quad (21)$$

The scattered field is defined as

$$\mathbf{U}^s(r, \varphi) = \sum_{m=0}^{\infty} \delta_m H_m^{(2)}(kr_0)(\mathbf{C}^{(m)} + \mathbf{D}^{(m)}) \times H_m^{(2)}(kr)\cos(m\varphi), \quad (22)$$

where

$$\mathbf{C}^{(m)} = \left\{-A_1\frac{J_m(ka)}{H_m^{(2)}(ka)}, -A_2\frac{J'_m(ka)}{H_m^{(2)\prime}(ka)}\right\}, \quad (23)$$

$$\mathbf{D}^{(m)} = \frac{2i(\mathbf{A}, \mathbf{M}^{(m)})\frac{n}{\varepsilon}J_m(kna)J'_m(kna)}{\pi ka H_m^{(2)}(ka)H_m^{(2)\prime}(ka)W^{(m)}}\mathbf{L}^{(m)}. \quad (24)$$

The directional pattern of scattered field $\mathbf{\Phi}^s(\varphi)$ can be written in the form of the series:

$$\mathbf{\Phi}^s(\varphi) = \sum_{m=0}^{\infty} \delta_m (i)^m H_m^{(2)}(kr_0) \times (\mathbf{C}^{(m)} + \mathbf{D}^{(m)})\cos(m\varphi). \quad (25)$$

Expressions (17) and (22) hold both for cylinders made of conventional materials ($\varepsilon > 0$, $\mu > 0$) and for cylinders made of metamaterials ($\varepsilon < 0$, $\mu < 0$). Refractive index n (see Eq. (16)) for these cases will be assumed positive.

Expansions (17) and (22) converge for any real values of parameters ε or μ, which can easily be proved using the Debye asymptotic representations for cylindrical functions J_m and $H_m^{(2)}$ for $m \longrightarrow \infty$ [15]. Function $W^{(m)}$ appearing in the denominators of expressions (19) and (24), which is a complex function of parameter ka, does not vanish for real values of frequency ka. For this reason, the problem of diffraction from a cylinder considered here has a solution for any real values of the parameters of the material (including $\varepsilon = \mu = -1$), while there is no solution to the problem of diffraction of the field of a pointlike source on half-space $\varepsilon = \mu = -1$ in the absence of heat loss [8].

We will consider only electrically small cylinders:

$$ka \ll 1, \quad nka \ll 1. \quad (26)$$

The denominators of expressions (17) and (22) contain resonance functions $W^{(m)}(ka)$ defined by formula (15). Let us analyze the frequency dependence of these denominators. If conditions (26) are satisfied, the real part of expression (15) considerably exceeds its imaginary part. The real part of functions $W^{(m)}(ka)$ vanishes at the points that are exactly the resonance frequencies. Thus, the equation for resonance frequencies has the form

$$\mathrm{Re}[W^{(m)}(ka)] = 0. \quad (27)$$

At resonance frequencies, single azimuthal harmonic $\cos(m\varphi)$ dominates in expansions (17) and (22).

Let us transform equality (27) using the asymptotic expressions of cylindrical functions for small values of the argument [15]:

$$J_m(x) = \frac{x^m}{2^m m!}\left[1 - \frac{x^2}{4(m+1)} + \ldots\right], \quad H_m^{(2)}(x) = \frac{i2^m(m-1)!}{\pi x^m}\left[1 + \frac{x^2}{4(m-1)} + \ldots\right], \quad m \geq 2. \quad (28)$$

Taking into account these expressions and retaining in Eq. (27) the zeroth- and first-order terms in the pow-

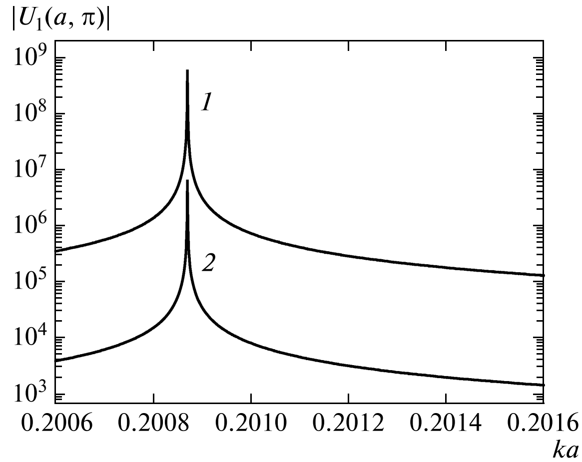

Fig. 2. Amplitude–frequency characteristic of an anisotropically conducting cylinder made of a metamaterial with $\varepsilon = -1.3$, $\mu = -1.00009775$, $\psi = 1.3$, $A_1 = 1$, $A_2 = 0$ (*1*) and $A_1 = 0$, $A_2 = 1$ (*2*).

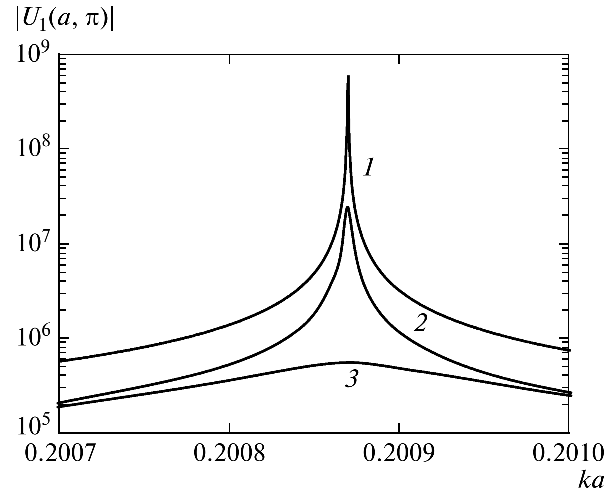

Fig. 3. Amplitude–frequency characteristic of an anisotropically conducting cylinder made of a metamaterial with $\varepsilon' = -1.3$, $\mu = -1.00009775$, $\psi = 1.3$ for different values of dielectric loss: $\varepsilon'' = 10^{-8}$ (*1*), 10^{-7} (*2*), and 10^{-5} (*3*).

ers of small parameter $(ka)^2$, we obtain the following expression for resonance frequencies:

$$(ka)^2 = \frac{\left(1 + \dfrac{1}{\mu}\right)\sin^2\psi}{\dfrac{1+\varepsilon}{m^2}\cos^2\psi + \dfrac{1}{2m}\left(\dfrac{1}{m-1} + \dfrac{\varepsilon}{m+1}\right)\sin^2\psi}, \quad (29)$$

$$m \geq 2.$$

It should be recalled that this expression holds only when condition $ka \ll 1$ is satisfied. To this end, it is necessary that any of the following inequalities be satisfied:

$$\psi \ll 1, \quad (30)$$

$$|\mu + 1| \ll 1. \quad (31)$$

For $\psi \ll 1$, formula (29) is also applicable for a cylinder made of a conventional material ($\varepsilon > 0$, $\mu > 0$). For a metamaterial, the right-hand side of relation (29) can be small in view of the fulfillment of condition (31). In this case, formula (29) is valid for structures with any twist angles of the conductivity helical lines.

3. NUMERICAL RESULTS

The numerical results presented below were obtained by summing series (17) and (22) as well as by using the modified method of discrete sources [16, 17]. The results of calculations obtained by these two methods coincide.

Calculations were performed in the range of parameters satisfying conditions (26) and (31). In all calculations, the coordinate of the source was assumed to be $r_0 = 1.2a$.

Let us analyze the amplitude–frequency characteristic (AFC) of a cylinder, i.e., the dependence of the field modulus at point $r = 0.99a$, $\varphi = \pi$ on dimensionless parameter ka proportional to frequency. Figure 2 shows the AFC for $\varepsilon = -1.3$, $\mu = -1.00009775$, and $\psi = 1.3$. Curves *1* and *2* correspond to AFCs of the cylinder for two conditions of excitation. The figure shows the graphs only for component U_1 since the values of component U_2 turned out to be two orders of magnitude smaller. Curve *1* in this figure corresponds to excitation by an electric current filament ($A_1 = 1$, $A_2 = 0$), while curve *2* corresponds to excitation by a magnetic current filament ($A_1 = 0$, $A_2 = 1$). Comparison of curves *1* and *2* shows that the efficiency of excitation of oscillations in the cylinder by the magnetic current is two orders of magnitude lower than in the case of electric current filament. For this reason, we will consider only component U_1, assuming that $A_1 = 1$, $A_2 = 0$. Calculations show that at resonance frequency $ka = 0.20087$, the field on the cylinder surface and the scattering diagram are described by a single harmonic $\cos(5\varphi)$ with large amplitudes on the order of 10^8 and 10^4, respectively.

To analyze the effect of heat loss on the Q factor of resonances, we will use the modified discrete source method [16, 17]. Figure 3 shows the family of curves describing the AFCs of the structure under investigation in the vicinity of resonance frequency $ka = 0.20087$ for various values of ε'' determining the dielectric loss in the medium ($\varepsilon = \varepsilon' - i\varepsilon''$). It can be seen from the figure that an increase in the heat loss leads to a decrease in the Q factor of resonance:

$$Q = \frac{ka}{\Delta ka_{0.7}}$$

($\Delta ka_{0.7}$ is the width of the resonance curve at a level of 0.707). Curve *1* in Fig. 3 ($\varepsilon'' = 10^{-8}$) almost coincides with curve *1* in Fig. 2, corresponding to zero heat loss

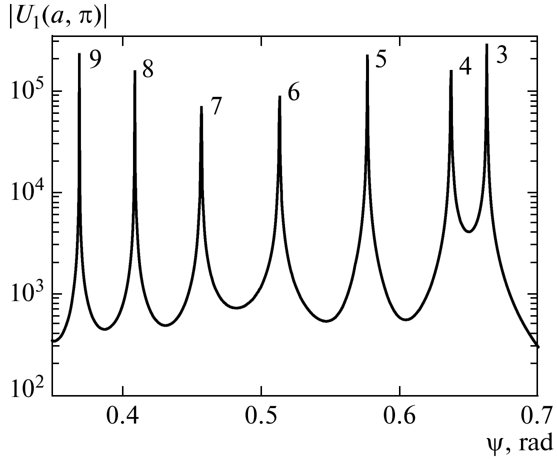

Fig. 4. Dependence of the modulus of field $U_1(a, \pi)$ on the spiral twist angle for $ka = 0.2...$, $\varepsilon = -1.3$, $\mu = -0.999$; numbers correspond to azimuth index m of the resonance.

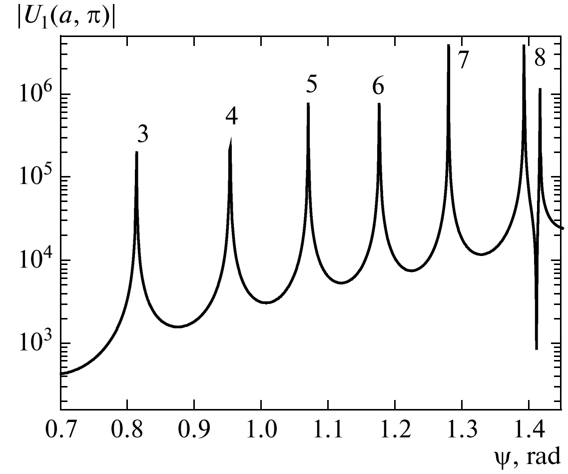

Fig. 5. Dependence of the modulus of field $U_1(a, \pi)$ on the spiral twist angle for $ka = 0.2...$, $\varepsilon = -1.3$, $\mu = -0.99999$; numbers correspond to azimuth index m of the resonance.

($Q \sim 10^6$). For $\varepsilon'' = 10^{-5}$, the Q factor decreases to $Q \sim 10^3$.

It should be noted that for an arbitrary spiral angle ψ in the frequency range of ka, resonance may not be attained. Resonances appear only when angles ψ lie in narrow intervals near certain discrete values ψ_m, and these discrete values correspond to resonances with various azimuth indices m. To clarify this situation, Figures 4–6 show the dependences of field modulus $U_1(r, \varphi)$ at point $r = 0.99a$, $\varphi = \pi$ on the spiral twist angle at frequency $ka = 0.20087$ for three values of permeability $\mu + 1 = 10^{-5}$, 10^{-4}, and 10^{-3}. The permittivity in this case was $\varepsilon = -1.3$. It can be seen that the curves in Figs. 4–6 are of the resonance nature. The index of resonance angle ψ_m coincides with the number of the azimuthal harmonic dominating in the field of the resonance oscillation. Note that for $\mu + 1 = 10^{-5}$ (Fig. 5), resonance angles ψ_m increase with number m, and for $\mu + 1 = 10^{-3}$ (Fig. 4), resonance angles decrease with increasing m. For $\mu + 1 = 10^{-4}$, the monotonic dependence on the number disappears, and pairs of resonances ψ_m with numbers 4 and 9, 8 and 5, and 7 and 6 converge, forming "doublets" (see Fig. 6).

Let us prove that such a behavior of the resonance parameters is associated with the intersection of the dispersion curves corresponding to different azimuth indices m (i.e., with degeneracy of oscillations). Figure 7 shows a family of curves describing the relation between the resonant value of twisting angle ψ_m and permeability μ of the cylinder for $ka = 0.2...$ and $\varepsilon = -1.3$. Different curves correspond to different values of azimuth index m. The curves in Fig. 7 are the trajectories of the peak of the field modulus in the 2D domain (ψ, μ) for preset values of ka and ε. The curves were obtained as a result of calculations based on expression (17) in the vicinity of resonant spikes of the wave field. Solid and dotted curves correspond to positive and negative values of quantity $1 + \mu > 0$, respectively. Figure 7 shows that there exist a domain of parameter $1 + \mu$ in which the dispersion curves intersect.

It should be noted that the dependences of permeability on the twist angle plotted using formula (29) coincide with the curves in Fig. 7 with graphical accuracy.

Let us analyze the spatial structure of the resonance field for parameters $\mu = -0.9999...$ and $\psi = 0.899...$, which ensure degeneracy of oscillations with azimuth indices $m = 4$ and 9. Figure 8 shows the field distribution over the cylinder surface, described by function $\cos(9\varphi)$. Figure 9 shows the scattering diagram for the cylinder under investigation; it contains only one harmonic $\cos(4\varphi)$. Figure 10 shows the distribution of

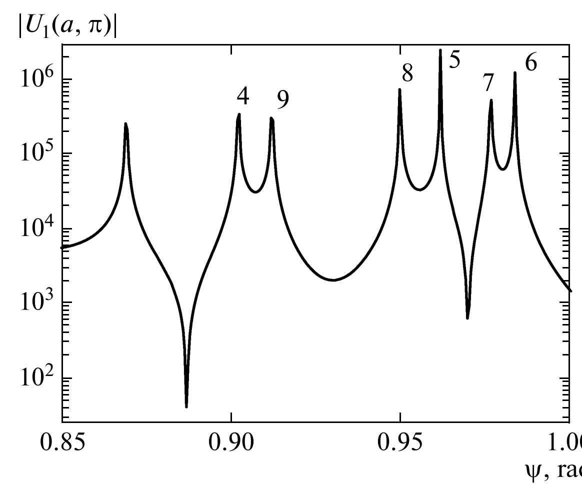

Fig. 6. Dependence of the modulus of field $U_1(a, \pi)$ on the spiral twist angle for $ka = 0.2...$, $\varepsilon = -1.3$, $\mu = -0.9999$; numbers correspond to azimuth index m of the resonance.

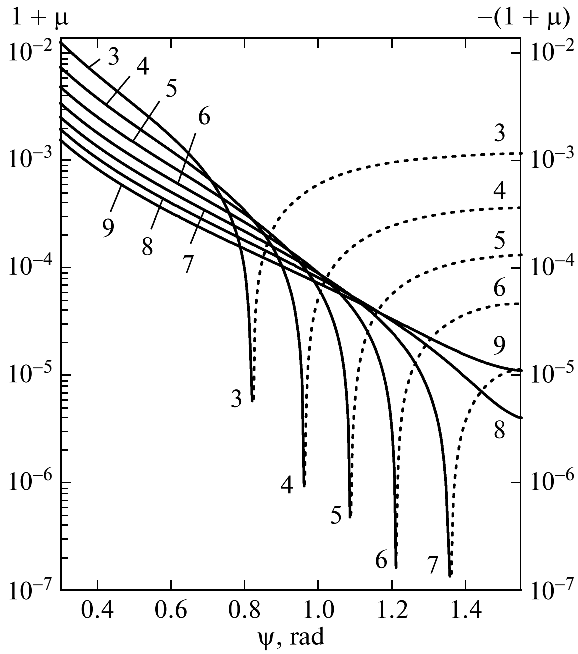

Fig. 7. Trajectories of resonance parameters of modes with index m in the (μ, ψ) plane for $ka = 0.2...$, $\varepsilon = -1.3$; numbers correspond to azimuth index m of the resonance. Solid curves correspond to $1 + \mu > 0$ (left scale); dotted curves correspond to $1 + \mu < 0$ (right scale).

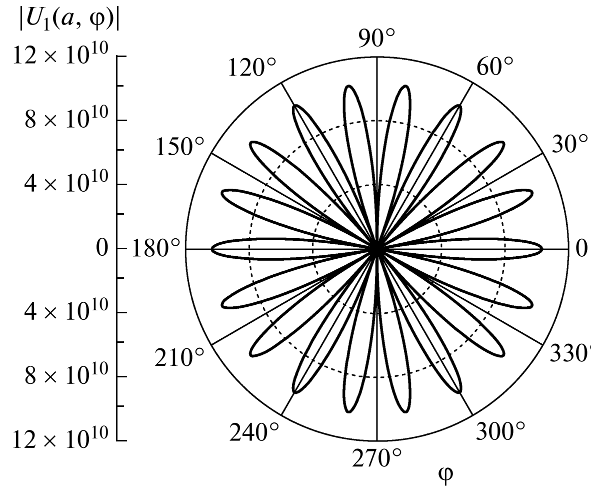

Fig. 8. Distribution of the modulus of field $U_1(a, \varphi)$ at degeneracy point 4, 9 for $ka = 0.2...$, $\varepsilon = -1.3$, $\mu = -0.999895...$, $\psi = 0.8993626...$.

total field modulus $|U_1|$ over the radial coordinate (along direction $\varphi = \pi$). It can be seen that the curve contains three segments, $kr < 0.6$, $0.6 < kr < 3$, and $kr > 0.3$, on which the field is described by functions $|U_1| \sim (kr)^{-9}$, $|U_1| \sim (kr)^{-4}$, and $|U_1| \sim (kr)^{-1/2}$, respectively. The first segment corresponds to the near field, in which the harmonic with $m = 9$ dominates. The second segment also corresponds to the near field, but with a dominant harmonic with $m = 4$. Finally, the third segment corresponds to the far field.

Figure 11 gives a general idea about the spatial distribution of field modulus $|U_1|$ on plane (x, y). It should be borne in mind that the difference in the field amplitudes in the spatial region under investigation is quite large (see also Fig. 10). It can be seen that in the vicinity of the cylinder ($kr \approx 0.2$), the interference pattern contains 18 radial fringes; for $kr > 0.7$, the number of fringes decreases to eight.

In the vicinity of point $kr \approx 0.6$ (Fig. 10), the laws of the decrease in the resonance field in the radial coordinate change. In the annular region $0.5 < kr < 0.7$, a complex interference pattern emerges as a result of summation of two harmonics $\cos(4\varphi)$ and $\cos(9\varphi)$ with commensurate amplitudes, which results in a complex interference pattern.

It should be emphasized that the fields behave analogously at all degeneracy points (i.e., at the points of intersection of the curves shown in Fig. 7); namely, the higher azimuthal harmonic dominates in the field on the contour, and the lower harmonic dominates in the far field.

4. STRUCTURE OF RESONANCE FIELDS IN THE STATIC REGION

Let us consider in greater detail the spatial and polarization structures of fields in the resonance conditions. The resonances described in the previous section are quasi-static. The electromagnetic field is concentrated in the static region $kr \ll 1$ and rapidly attenuates with increasing distance from the cylinder surface. In this region, electromagnetic field components E_z and H_z approximately satisfy the Laplace equation. We can easily obtain the following expressions for oscillations with number m in the quasi-static approximation:

$$E_z = \begin{cases} \dfrac{ka}{m}\left(\dfrac{r}{a}\right)^{m} \exp(im\varphi), & r < a, \\ \dfrac{ka}{m}\left(\dfrac{r}{a}\right)^{-m} \exp(im\varphi), & r > a, \end{cases} \tag{32}$$

$$E_r = \begin{cases} i\dfrac{ka}{m}\cot\psi\left(\dfrac{r}{a}\right)^{m-1} \exp(im\varphi), & r < a, \\ -i\dfrac{ka}{m}\cot\psi\left(\dfrac{r}{a}\right)^{-m-1} \exp(im\varphi), & r > a, \end{cases} \tag{33}$$

$$E_\varphi = \begin{cases} -\dfrac{ka}{m}\cot\psi\left(\dfrac{r}{a}\right)^{m-1} \exp(im\varphi), & r < a, \\ -\dfrac{ka}{m}\cot\psi\left(\dfrac{r}{a}\right)^{-m-1} \exp(im\varphi), & r > a, \end{cases} \tag{34}$$

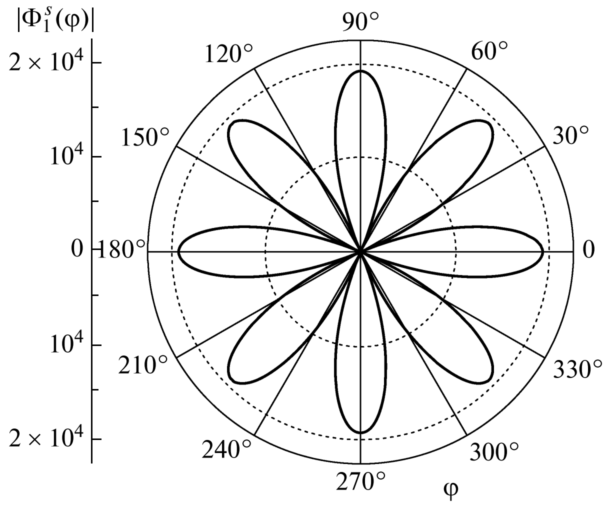

Fig. 9. Modulus of scattering diagram $\Phi_1^s(\varphi)$ of the field on the cylinder at degeneracy point 4, 9 for $ka = 0.2...$, $\varepsilon = -1.3$, $\mu = -0.999895...$, $\psi = 0.8993626...$.

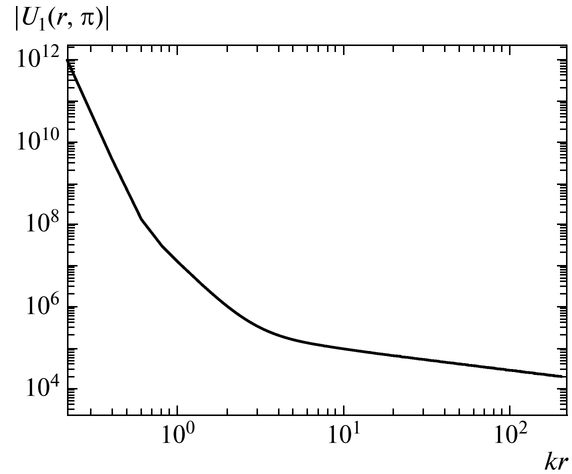

Fig. 10. Distribution of the modulus of field $U_1(r, \varphi)$ outside the cylinder at degeneracy point 4, 9 for $ka = 0.2...$, $\varepsilon = -1.3$, $\mu = -0.999895...$, $\psi = 0.8993626...$.

$$H_z = \begin{cases} i\left(\dfrac{ka}{m}\right)^2 \varepsilon\cot\psi\left(\dfrac{r}{a}\right)^m \exp(im\varphi), & r < a, \\ -i\left(\dfrac{ka}{m}\right)^2 \cot\psi\left(\dfrac{r}{a}\right)^m \exp(im\varphi), & r > a, \end{cases} \tag{35}$$

$$H_r = \begin{cases} -\dfrac{1}{\mu}\left(\dfrac{r}{a}\right)^{m-1} \exp(im\varphi), & r < a, \\ -\left(\dfrac{r}{a}\right)^{-m-1} \exp(im\varphi), & r > a, \end{cases} \tag{36}$$

$$H_\varphi = \begin{cases} -\dfrac{i}{\mu}\left(\dfrac{r}{a}\right)^{m-1} \exp(im\varphi), & r < a, \\ i\left(\dfrac{r}{a}\right)^{-m-1} \exp(im\varphi), & r > a, \end{cases} \tag{37}$$

The electric field defined by formulas (32)–(34) satisfies the electrostatics equation

$$\operatorname{div}\mathbf{E} = 0 \tag{38}$$

and boundary conditions (1). The magnetic field (35)–(37) with allowance for conditions (31) approximately satisfies both the magnetostatics equation

$$\operatorname{div}\mathbf{H} = 0 \tag{39}$$

and boundary condition (2). Expressions (32)–(37) also satisfy relations (7) and (8).

It should be noted that the spiral twist angle ψ is assumed to be small; consequently $\cot\psi$ cannot assume large values. Therefore, with allowance for condition $ka \ll 1$, we conclude that the magnetic component $|\mathbf{H}| \gg |\mathbf{E}|$ dominates in field (32)–(37). In this case, the following relations hold:

$$|E_z| \gg |H_z|, \tag{40}$$

$$|H_r| = |H_\varphi| \gg |H_z|. \tag{41}$$

Thus, we can assume that the magnetic field is perpendicular to the z axis (see Fig. 1). Condition (40) (i.e., $|U_1| \gg |U_2|$) matches the results of numerical calculations given in the previous section.

Let us consider the polarization structure of the fields of self-oscillations. Formulas (32) and (34) imply that the electric field component tangential to cylindrical surfaces $r = \text{const}$ has the linear polarization; in this case, we have

$$\frac{E_\varphi}{E_z} = -\frac{a}{r}\cot\psi. \tag{42}$$

Thus, the electric field lines on the cylinder surface $r = \text{const}$ are helical. It follows from relation (42) that these lines on the boundary $r = a$ of a metamaterial cylinder are orthogonal to the spiral conductors. When radius r increases, the twist angle of the electric field lines decreases.

The electric and magnetic field components lying in the planes perpendicular to the cylinder axis are circularly polarized: $E_r = \pm iE_\varphi$, $H_r = \pm iH_\varphi$. Inside and outside the cylinder $r = a$, these fields with the circular polarization have opposite directions of rotation. These properties are typical of chiral objects [13].

The equation for the eigenfrequencies of quasi-static oscillations can be derived from the following relation expressing the equality of the energies stored

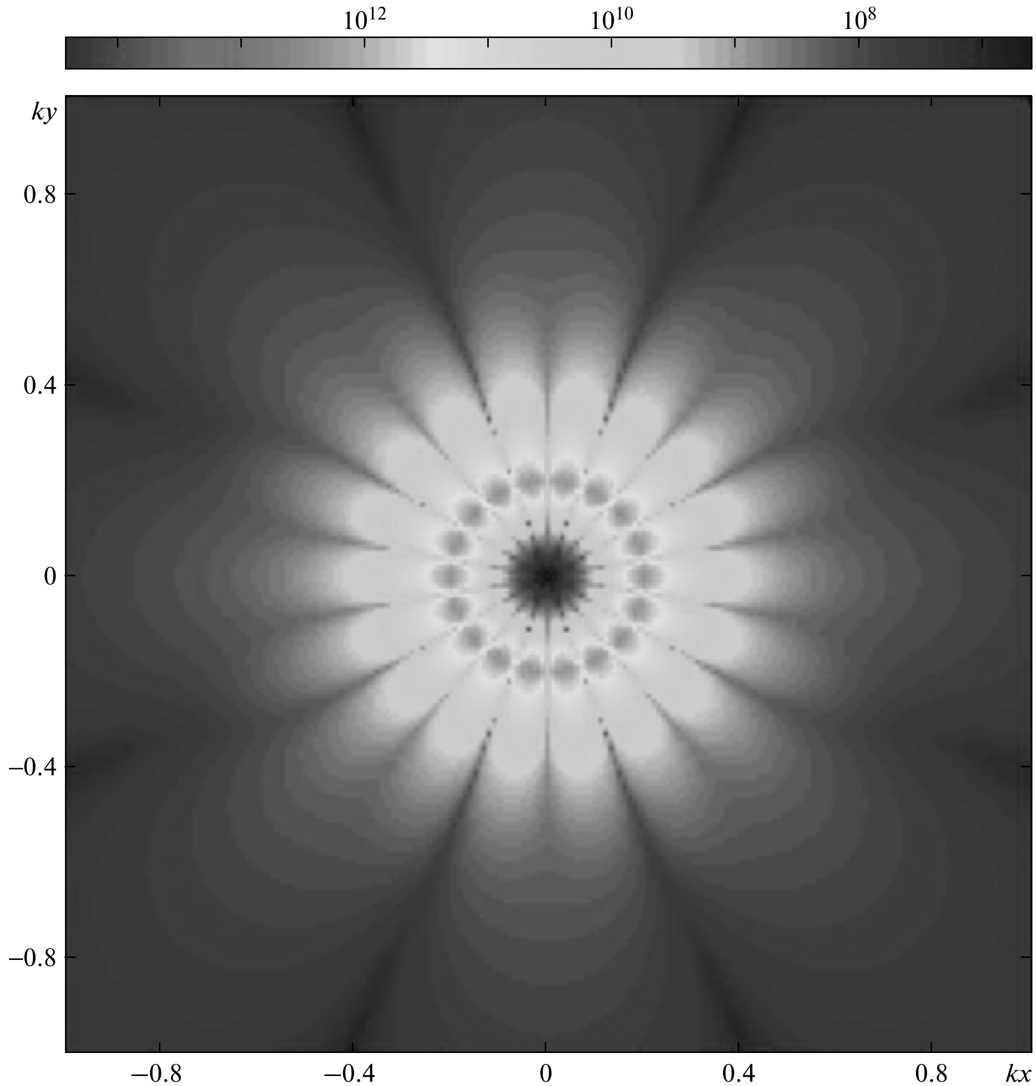

Fig. 11. Spatial distribution of function $|U_1|$ in the (x, y) plane for $ka = 0.2\ldots$, $\varepsilon = -1.3$, $\mu = -0.999895\ldots$, $\psi = 0.8993626\ldots$.

by the electric and magnetic fields of the resonant structure under investigation:

$$\int_0^{\infty}\int_0^{2\pi}\mu(r)[|H_r(r,\varphi)|^2 + |H_\varphi(r,\varphi)|^2]rdrd\varphi$$
$$= \int_0^{\infty}\int_0^{2\pi}\varepsilon(r)[|E_z(r,\varphi)|^2 + |E_r(r,\varphi)|^2 + |E_\varphi(r,\varphi)|^2]rdrd\varphi. \tag{43}$$

This property is well known from the theory of bulk resonators [18]. In formula (43), we have disregarded component H_z in view of relation (41). Since the electromagnetic field is concentrated in the static region, we can use formulas (32)–(34), (36), and (37) in (43). Performing integration, we obtain Eq. (29). Thus, this equation is equivalent in physical meaning to the Thomson formula $\omega^2 = 1/LC$, which determines the resonance frequency of the LC circuit.

5. CONCLUSIONS

We have numerically investigated the excitation of a cylindrical multiturn wire helix filled with a metamaterial by filaments of electric and magnetic currents. In cylinders small as compared to the wavelength and having a permittivity close to −1, the effect of degeneracy of high-Q resonators has been observed.

We have analyzed the dynamics of degeneracy of self-oscillations of a chiral cylinder filled with a metamaterial. It has been shown that there exist oscillations for which the azimuthal dependence $\cos(m\varphi)$ of the field has different values of index m in near and far fields. Resonances have been described analytically in the quasi-static approximation. An explicit expression has been derived for eigenfrequencies of a cylindrical chiral cylinder filled with a metamaterial.

ACKNOWLEDGMENTS

This study was supported in part by the Russian Foundation for Basic Research (project no. 12-02-00062-a).

REFERENCES

1. V. G. Veselago, Sov. Phys.—Usp. **10** (4), 509 (1967).
2. K. Yu. Bliokh and Yu. P. Bliokh, Phys.—Usp. **47** (4), 393 (2004).
3. D. R. Smith, J. B. Pendry, and M. C. K. Wiltshire, Science (Washington) **305**, 788 (2004).
4. A. A. Zharov, I. G. Kondrat'ev, and A. I. Smirnov, Izv. Vyssh. Uchebn. Zaved., Radiofiz. **48**, 978 (2005).
5. A. B. Petrin, JETP Lett. **87** (9), 464 (2008).
6. A. A. Zharov, N. A. Zharova, and R. E. Noskov, J. Exp. Theor. Phys. **109** (5), 734 (2009).
7. A. Sihvola, Metamaterials **1**, 2 (2007).
8. A. P. Anyutin, I. P. Korshunov, and A. D. Shatrov, J. Exp. Theor. Phys. **118** (1), 27 (2014).
9. V. V. Klimov, Opt. Commun. **211**, 183 (2002).
10. A. P. Anyutin, I. P. Korshunov, and A. D. Shatrov, in *CD-ROM Proceedings of the Seventh International Congress on Advanced Electromagnetic Materials in Microwaves and Optics (Metamaterials'2013), Bordeaux, France, September 16–21, 2013* (Bordeaux, 2013), p. PSIII25.
11. A. P. Anyutin, I. P. Korshunov, and A. D. Shatrov, J. Commun. Technol. Electron. **59** (5), 400 (2014).
12. D. V. Guzatov and V. V. Klimov, New J. Phys. **14**, 123009 (2012).
13. B. Z. Katsenelenbaum, E. N. Korshunova, A. N. Sivov, and A. D. Shatrov, Phys.—Usp. **40** (11), 1149 (1997).
14. I. P. Korshunov, E. N. Korshunova, A. N. Sivov, and A. D. Shatrov, J. Commun. Technol. Electron. **52** (4), 365 (2007).
15. M. Abramowitz and I. A. Stegun, *Handbook of Mathematical Functions: With Formulas, Graphs, and Mathematical Tables* (Dover, New York, 1965; Nauka, Moscow, 1979).
16. A. G. Kyurkchan, S. A. Minaev, and A. L. Soloveichik, J. Commun. Technol. Electron. **46**, 615 (2001).
17. A. P. Anyutin, A. G. Kyurkchan, and S. A. Minaev, J. Commun. Technol. Electron. **47** (8), 864 (2002).
18. B. Z. Katsenelenbaum, *High-Frequency Electrodynamics* (Wiley, Weinheim, 2006).

Translated by N. Wadhwa